

Article

Towards Distributed Recycling with Additive Manufacturing of PET Flake Feedstocks

Helen A. Little¹, Nagendra G. Tanikella², Matthew J. Reich², Matthew J. Fiedler¹, Samantha L. Snabes¹, and Joshua M. Pearce^{2,3,4*}

¹ re:3D Inc., 1100 Hercules STE 220, Houston, TX, 77058, USA;

helen@re3d.org (H.A.L.); matthew@re3d.org (M.J.F.); samantha@re3d.org (S.L.S.)

³ Department of Material Science and Engineering, Michigan Technological University, Houghton, MI, 49931, USA; ngtanike@mtu.edu (N.G.T.); mjreich@mtu.edu (M.J.R.)

⁴ Department of Electrical and Computer Engineering, Michigan Technological University, Houghton, MI, 49931, USA

⁵ Department of Electronics and Nanoengineering, School of Electrical Engineering, Aalto University, Espoo, 00076, Finland

* Correspondence: pearce@mtu.edu; joshua.pearce@aalto.fi Tel.: +01-906-487-1466

Abstract: This study explores the potential to reach a circular economy for post-consumer recycled polyethylene terephthalate (rPET) packaging and bottles by using it as a distributed recycling for additive manufacturing (DRAM) feedstock. Specifically, rPET is processed using only an open source toolchain with fused particle fabrication (FPF) or fused granular fabrication (FGF) processing. In this study, first the impact of granulation, sifting and heating (and their combination) is quantified on the shape and size distribution of the rPET flakes. Then feeding studies were performed to see if they could be printed through an external feeder or needed to be direct printed with a hopper using two Gigabot X machines, one with extended part cooling and one without. Print settings were optimized based on thermal characterization and for the latter which was shown to print rPET directly from shredded water bottles mechanical testing is performed. The results showed that geometry was important for extended feeding tubes and direct printed using a hopper. Further there is a wide disparity in the physical properties of rPET from water bottles depending on source and the history of the material. Future work is needed to enable water bottles to be used as a widespread DRAM feedstock.

Keywords: polymers; recycling; waste plastic; upcycle; circular economy; PET; additive manufacturing; distributed recycling; distributed manufacturing; 3D printing

1. Introduction

The vast majority of plastics end up land filled or contaminating the natural environment as the global polymer recycling rate is an embarrassingly low 9% [1]. The problems of plastic recycling were recently highlighted when China imposed an import ban on waste plastic [2], which stalled global recycling efforts [3–5]. Without China, large-scale centralized plastic recycling has become uneconomic in

many cases and many municipalities have stopped recycling [6]. Part of the problem is that it is costly to separate the numerous types of plastic and as consumers have no direct financial incentive to do it in conventional centralized recycling, so increasingly sophisticated sorting technologies are proposed [7] to reach a circular economy [8–10].

Another approach to reach a circular economy for plastic is distributed recycling for additive manufacturing (DRAM) [11–13]. In the DRAM methodology consumers have an economic incentive [11,13] to recycle because they can use their waste as feedstock for a wide-range of consumer products that can be produced for a fraction of conventional costs of equivalent products [14–17]. DRAM is a new technology that has the potential to radically impact global value chains [18]. Early DRAM work was centered on open source waste plastic extruders known as recyclebots, which upcycled post-consumer plastic waste into 3-D printing filament [19,20]. In addition to reducing 3-D printing costs by several orders of magnitude, it decreased embodied energy of 3-D printing filament by 90% [21–23]. The open source 3-D printing community, having evolved from the self-replicating rapid prototyper (RepRap) model [24–26] have embraced open source methods to recycle 3-D printing waste [27] particularly for the two most popular fused filament materials: polylactic acid (PLA) [28–31] and acrylonitrile butadiene styrene (ABS) [11,32–35]. More common thermoplastics were more challenging but have been successfully converted to filament including high-density polyethylene (HDPE) [19,36,37], polypropylene (PP) and polystyrene (PS) [37], thermoplastic polyurethane (TPU) [38]; linear low density polyethylene (LLDPE) and low density polyethylene (LDPE) [39], polycarbonate (PC) [40]. Each melt and extrude cycle of a recyclebot impairs the mechanical properties of PLA [29], HDPE [41], and even of polyethylene terephthalate (PET) [42]. This limits the recycling cycles to about five [29] before reinforcement or blending with virgin materials become necessary. Polymer composites using carbon reinforced plastic [43], fiber filled composites [44,45], and various types of waste wood [46,47] have been used in recyclebot systems and more complex DRAM systems can use 3-D printed PC as molds for intrusion molding [40] for windshield wiper composites [48] as well as acrylonitrile styrene acrylate (ASA) and stamp sand waste composites [49]. Zander et al. [50] has studied PET, PP, and PS blends with styrene ethylene butylene styrene (SEBS) and maleic anhydride compatibilizers that were able to increase tensile strength from 19 MPa to 23 MPa, although pure recycled PET had the highest tensile strength of 35 MPa.

This is part of the reason that the holy grail of DRAM, however, has been PET. Although PET is only the 6th most commonly produced plastic, it has achieved this status because it is one of the most easily identifiable polymer waste streams for consumers [1] and is already widely recycled through centralized processes [51]. Although, the majority of centralized recycling is downcycling [52], and as noted earlier not nearly at the rate to drive a circular economy. PET is an excellent water and moisture barrier so it is used extensively in the packaging industry for consumable packaging of water and soft drinks as well as foods [53]. PET use is expected to maintain a growth rate of 4.5%/year [54]. PET water bottles are easy to

envision recycling at home as they are already clean and they are available in such large quantities globally as more than a million plastic bottles are produced every minute [55]. A few companies sell PET filament for 3-D printing including Verbatim, MadeSolid, and Ultrafuse and a few others sell recycled PET filament including Refil and B-PET. Although, recycled PET and PETG filament is available commercially [56,57], some companies have stopped production [58,59]. PET is less popular than PLA, ABS, and PETG (glycol modified version of PET) because the printing process is more challenging as PET has shrinkage and warpage issues from high fusion temperature and lack of control of crystallinity, water absorption (leading to molecular weight reduction), and weak interfacial welding between layers [60]. In the past, PET industrial waste has been shown to successfully print with fused particle fabrication (FPF) or fused granular fabrication (FGF) 3-D printers that fabricate products directly from chips [61].

In centralized recycling, contamination and moisture are the major causes of deterioration of both the physical and chemical properties of PET [51]. In fact, Awaja and Patel state that to make a food grade PET, the recycled PET must be hydrolyzed, purified, and re-polymerized [51]. Packaging-grade PET, has been thought to require an increase in the viscosity or decrease of the melt flow index for effective use in material extrusion AM. One way to approach this is to use pyromellitic dianhydride chain extenders to increase the melt flow index of rPET via reactive extrusion [62]. There have been sporadic claims of PET recycling in the maker community, but they have failed to gain traction the way PLA or ABS recycling has caught on primarily due to challenges in reproducibility. Part of these challenges also stem from the differences in the water bottles themselves, which are under constant flux. For example, since 2000, the average weight of a 16.9-ounce PET plastic bottle has declined by nearly half to 9.89 grams, saving billions of pounds of PET resin [63]. The largest problem, however, has been identified as PET undergoes hydrolytic degradation during melt processing, resulting in reduced molecular weights and if the feedstock is too wet even total disintegration of the polymer. Fortunately, there has been progress, as Tech4Trade and other partners developed a complex custom recyclebot (the Thunderhead) specifically for PET recycling [64,65]. This system not only has a complex number and sophisticated heating zones, it also has a heated hopper to ensure that the feedstock flakes are always dry. The first systematic study of PET-based DRAM was conducted by Zander et al. in 2018 [60]. They found that the chemistry for different PET feedstocks was identical, and their rheological results showed drying of the PET led to an increase in the viscosity [60]. Moreover, by altering the processing parameters they were able to control crystallinity (24.9% for no active cooling down to 12.2% for the water-cooled filament) [60]. Finally, Zander et al.'s results of a PET tensile strength of 35.1 ± 8 MPa was found to be extremely promising as a material for DRAM [60].

To build on these promising results, this study explores the potential of PET packaging as a DRAM feedstock further by using only an open source toolchain with FPF/FGF processing. Earlier work showed PET chips were processible [61], here the more challenging flakes from PET are investigated carefully for FPF/FGF processing.

In this study, first the impact of granulation, sifting, and heating is quantified on the shape and size distribution of the rPET flakes and pellets. Then a feeding study was performed to see if they could be printed through a feed tube connected to an externally mounted hopper, or if the flake needed to be direct printed with a gravity-fed hopper mounted to the print head. Two Gigabot X beta machines were used: one with extended part cooling and one without. Print settings were optimized based on DSC testing for the latter, and mechanical testing was performed. Both types of Gigabot X printers were used to fabricate products from rPET as examples. The results are presented and discussed in the context of future work to make water bottles a DRAM feedstock.

2. Materials and Methods

2.1 Materials

Two recycled PET (rPET) materials were tested (see Figure 1). First, Ultrafuse PET pellets, which have previously been shown to be conducive to FPF/FGF processing with a GigabotX prototype [61] with two hot zones were evaluated. This commercial recycled rPET was shown to have ideal temperature settings of 220 and 230°C for zone 1 and 2 respectively. The print bed was set at 100°C and printing speeds from 5-30 mm/s were all shown to be adequate [61]. The second material was flaked water bottles. To convert PET water bottles into 3-D printable regrind material, the labels, caps, and adhesives were removed before granulating the bottles in a SHINI USA open rotor scissor cut granulator [66]. The granulator produced regrind small enough to pass through its grate, which has 5.84 mm diameter holes. After granulation, the regrind was dried in a food dehydrator for 24 hours at 38°C. In Figure 1 the pellets (blue) are not only more uniform but also bulkier than the granulated water bottle rPET (clear granulate).



Figure 1. 50:50 mix of Ultrafuse (blue pellets) and shredded water bottle (clear) to show relative, size, shape and texture.

2.2 Granulate Particle Analysis

To compare the different PET sources, the granulate were characterized using FIJI ImageJ software [67]. The size characteristics of the particles for each starting material were quantified using digital imaging and the open source Fiji/ImageJ Circularity, c , was defined as [68]:

$$c = 4\pi \times \frac{A}{p^2} \quad (1)$$

Where A is area in mm and p is perimeter in mm. Thus, a circularity value of 1.0 indicates a perfect circle; whereas as the values approach 0, it indicates an increasingly elongated polygon. Then to compare the different processing methods for the PET water bottle granulate, the cross-sectional areas of granulate particles were plotted as normal distributions and compared.

2.3 rPET Thermal materials characterization

The thermal properties of rPET flake was first characterized with differential scanning calorimetry (DSC). rPET flake samples were tested three times using the Netzsch DSC 404 furnace under pure argon flow of 50 mL/min and a heating rate of 10°C/min. Background scans were performed on an empty aluminum crucible for each sample which generated calibration curves used to normalize the scan. The sample masses were measured with a precision of ± 0.01 mg on a Sartorius scale and then entered into the Netzsch software. During the tests, each PET sample was placed into the aluminum crucible pan alongside an empty reference pan, and then the furnace chamber was purged and backfilled with argon to ensure no oxygen was present. Following this, the instrument heated the pans starting at $30.0^\circ\text{C} \pm 7.5^\circ\text{C}$. Heating at a constant rate of 10°C per minute, the crucibles were brought to a temperature of 300°C, and then cooled back to room temperature.

2.4 FPF/FGF 3-D Printing

Two approaches were taken to print with flaked water bottles. In the first approach a feed tube arrangement (Figure 2a) was used with a 3-heat-zone Gigabot X (re:3D, Texas) (Figure 2b). In order to assess the ability for a material to print on Gigabot X beta design (Figure 2a), consistent flow through the printer's feeding system was evaluated. Therefore, all samples of processed granulate were subjected to feed tests to identify which samples flowed through both the feed tube and feed tube adapter. A testing device was built with these components (Figure 2c). To perform the feed test on a material sample the following steps were used:

1. Blocked bottom end of the feed tube
2. Loaded the feed tube from the top with test material until it is full
3. Unblocked the bottom of the feed tube to allow material to flow through via gravity
4. Recorded whether all the material flowed through or became stuck inside the tube
5. Repeated with the feed tube adapter attached at bottom of the feed tube to measure material flow through both the tube and adapter

To determine the printing temperatures and test the extrusion rate of PET granulate, the extruder was first flushed with Ultrafuse recycled PET (rPET) commercial pellets [69]. The PET water bottle granulate (flake) was then fed directly into the feed tube adapter to eliminate any effect of inconsistent granulate flow through the feed tube (Figure 2c). Initial extruder temperatures were set to 250°C for the bottom heating zone closest to the nozzle, 240°C for the middle, and 180°C for the top. The bottom zone temperature was set to the melting temperature of the granulate, and the top temperature was set low enough for the granulate at the top of the pellet screw to remain unmelted and provide pressure to extrude the melted plastic lower in the screw.

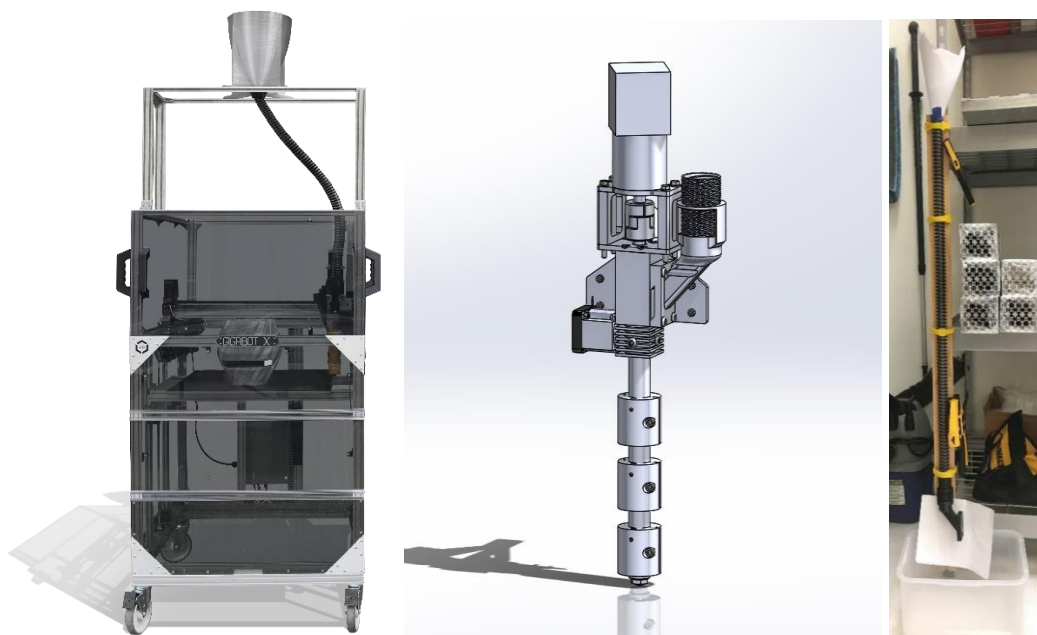


Figure 2. (a) GigabotX (beta) design with feed tube, (b) close up of 3-heat zone extruder, and (c) feed test apparatus.

To flush the Ultrafuse rPET pellets out of the extruder and transition to extruding the PET granulate, the extruder motor was rotated in increments of 200mm, at 600 steps/mm and at a speed of 3 mm/s. The use of millimeters in both the printer firmware and in Simplify3D, is designed for filament printing, and describes the length of filament pulled by the motor and extruded. When open source firmware and slicing is developed specifically for direct drive FPF these values can be converted to rotations per minute using the steps per revolution for the motor to be consistent with what is occurring physically. When flushing from rPET pellets to PET water bottle granulate, the granulate did not extrude reliably. When flushing from water bottle granulate to rPET pellets, consistent extrusion was achieved. This indicated feeding issues due to the physical particle characteristics.

Therefore, additional processing methods were explored to decrease particle size and increase particle sphericity. This is because it is well known that spherical particles flow most easily and although the impact of size on flow of particles is

complex, in this system the smaller the particle size would have a lower probability of becoming jammed and restricting flow in the feeding tube. These processing methods that were expected to improve feeding and printability include:

1. **Granulating Twice:** Feeding granulated water bottles back into the SHINI granulator [66].
2. **Sifting:** Sifting through a 3-D printed sifter [70] with holes 5mm in diameter and 2mm deep. Sifting removes 40% of the granulate by weight, producing a 60% yield.
3. **Heating:**
 - a. Heating in a food dehydrator at 65.5°C for 24 hours.
 - b. Heating in a Quincy Lab Analog Air Forced Lab Oven [71] at 100°C for 1 hour.
4. **Combined sifting (2) and heating (3b):** Sifted through the 5mm hole sifter, then heated in the oven at 100°C for one hour.

Additional tests were conducted to further quantify factors affecting particle shape when heated. Fiji/ImageJ measures a curled particle as having a smaller cross-sectional area than if the same particle were flattened. To better measure particle area changes without the factor of curling, flat 1" x 1" square samples (6.45cm²) were cut from the top portion of water bottles and submitted to various heating tests. To evaluate the diversity of plastic PET previously reported, five different brands of water bottles were assessed: Baraka, Hill Country Fair, Great Value, Ozarka, and Texas Music Water. Baraka bottles were sourced from a U.S. Air Force Forward Operating Base, and the others were sourced in Houston. Samples of each brand were heated at 100°C for 1 hour. After the heat cycle, dimensions were measured while the samples squares were flat. Tests for time and temperature dependence on plastic sample dimensions were also performed on water bottle brands Baraka (avg thickness 0.25 mm) and Ozarka (average thickness 0.2 mm):

1. Time dependence: heating at 100°C for varying lengths of time
2. Temperature dependence: heating for 5 mins at temperatures ranging from 60-100°C

A second approach was taken, which utilized the same single granulated water bottles used a direct feed hopper prototype Gigabot X consisting of 1.75mm printer nozzle diameter – and a 3-D printed cooling arrangement shown in Figure 3. The design files for the cooling setup can be found on the Open Science Framework [70].

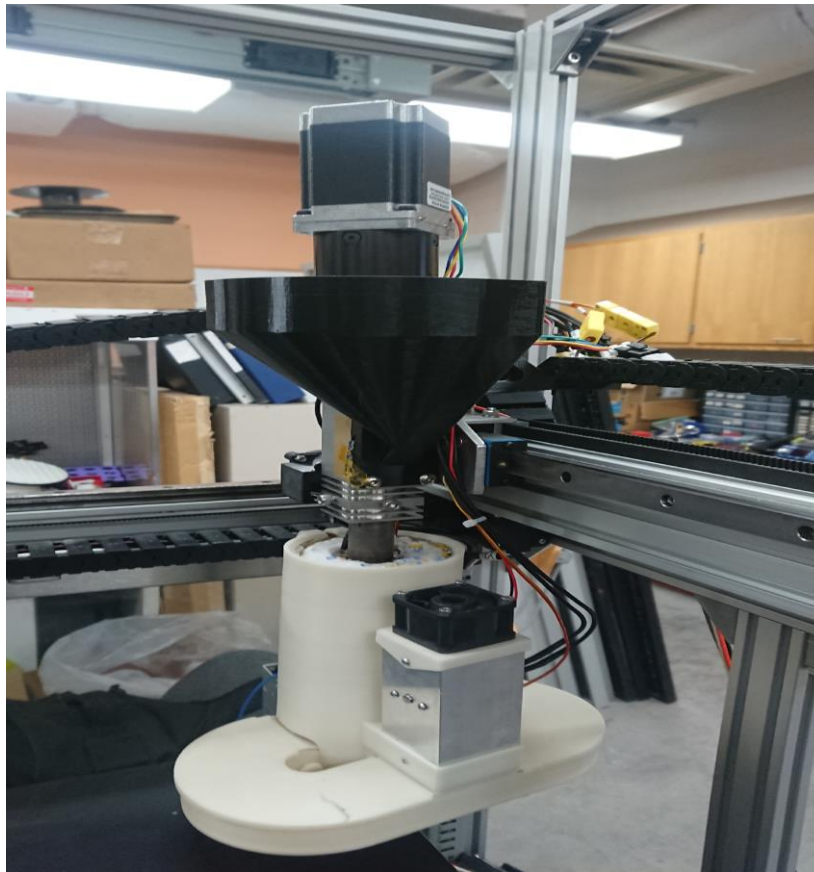


Figure 3. GigabotX with 3-D printed direct feed hopper (black) and 3-D printed cooling shroud (white) with the source code available [70].

2.5 Printing Settings Optimization

Using the direct feed, 3-D printed cooling setup in Figure 3, print optimization was done on two geometries:

1. Cylinder: 20mm diameter, 40mm length, slicer generated mass of 17.3 grams.
2. Cuboid: 50mm length, 50mm width, 5mm height, slicer generated mass of 17.3 grams.

Following similar protocols to those established by Woern et al. [61], optimization was done in the 180°C to 260°C region, with the heater region closer to the nozzle always having an equal or higher temperature. The minimum temperature at the top of the feeder was chosen based on the motor skipping. This indicates that the torque required to turn the extruder screw is higher than the extruder motor's torque output, which usually means material is unmelted or highly viscous. A temperature where no motor skipping was chosen (210°C). The maximum temperature close to the nozzle was chosen based on blob-like appearance of the print due to melting of the material (240°C). Specimens were printed at various temperature combinations in the selected "printable" region, and the chosen geometries were optimized based on visual quality and mass of the specimen. Three print speeds were tested: 10mm/s, 30mm/s and 50mm/s.

2.6 Mechanical Testing

Tensile testing was completed on the rPET using the ASTM D638 Type 1 standard tensile bars. The bars were printed at ideal print settings that were found during optimization of the cuboid at 100% infill. The infill pattern was set to 45 degrees with respect to the long axis of the tensile bars. Five (5) specimens were tested in each sample. The specimens were then pulled until failure using a 10kN load cell on an Instron 4210 Testing machine. The strain data was captured using the crosshead of the Instron 4210.

3. Results and Discussion

3.1. Particle Size Analysis of Granulate and Feeding

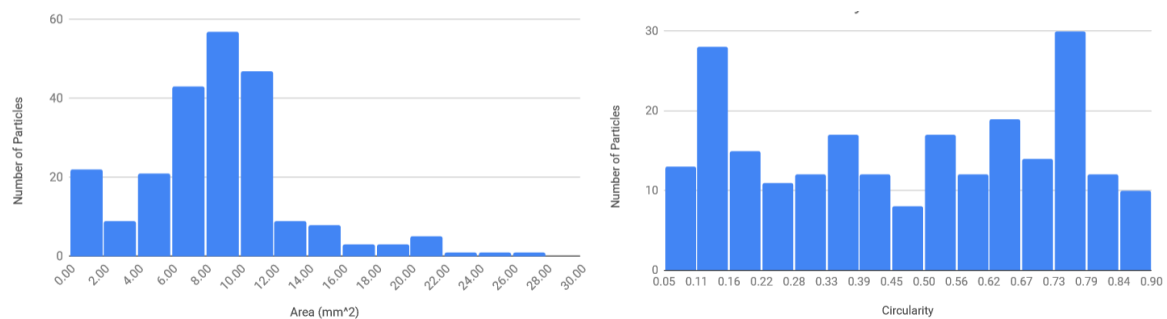


Figure 4. Ultrafuse rPET a) particle size distribution and b) particle circularity as a function of area.

For the Ultrafuse rPET pellets shown in Figure 4 the average area was 8.73 mm² and the median area was 8.57 mm² with a standard deviation of 4.59. The average circularity for the Ultrafuse rPET was 0.47, the median was 0.50 with a standard deviation of 0.25.

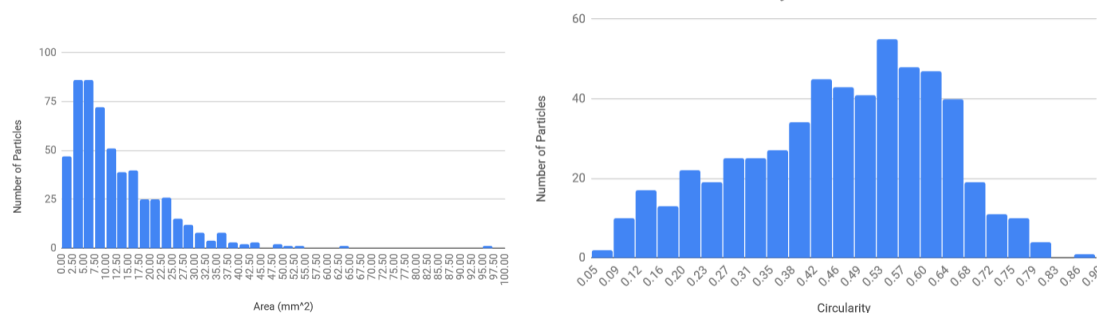


Figure 5. Houston-sourced PET water bottle flake a) particle size distribution, b) particle circularity and c) circularity as a function of area.

As can be seen in Figure 5 the average area was 12.56 mm² and the median area was 9.27mm² with a standard deviation of 10.43. The average circularity for the unscreened water bottle rPET was 0.47, the median was 0.49 with a standard deviation of 0.17.

By comparing the results of the two materials in Figure 4 and 5, the particle area of the Ultrafuse pellets is substantially smaller than the recycled water bottle granulate, as is the standard deviation. The circularity of the two materials is equivalent. A clear approach to improving the printability of the recycled water bottle PET is simply to reduce its size. The impact of the four approaches to reduce the size of the rPET water bottle granulate is shown in Figure 6.

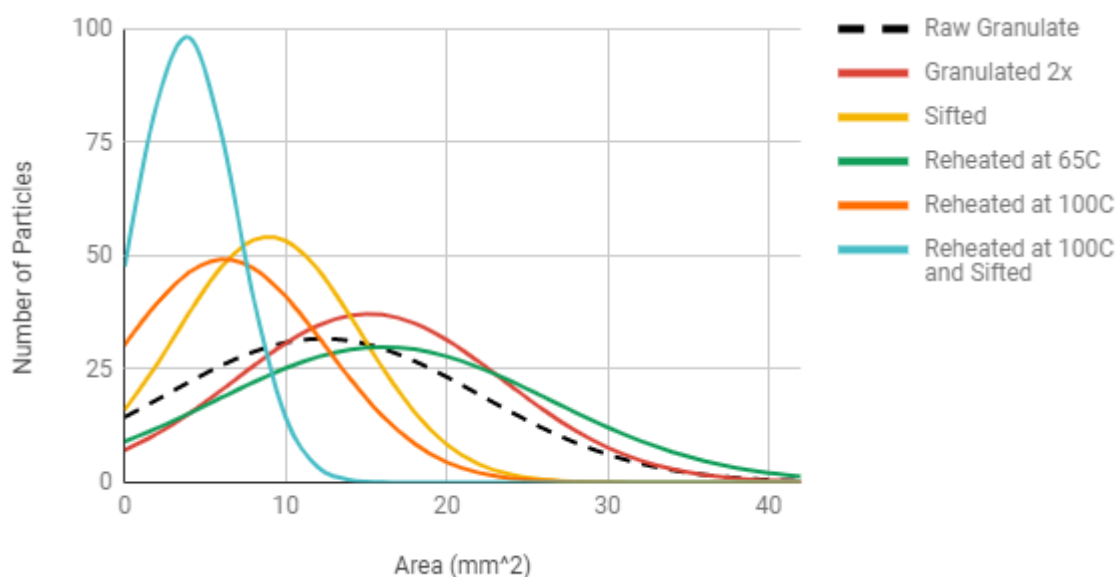


Figure 6: Effect of different processing methods on the normal distribution curves for PET water bottle granulate particle area.

As can be seen in Figure 6, the ImageJ particle analysis revealed the following conclusions for the different processing methods:

1. **Granulating Twice:** Passing the water bottle granulate through the SHINI granulator twice does not decrease particle size (Figure 6). In fact, it shifts the particle size distribution to the right, toward larger particles. This indicates a loss of smaller particles ($< 2 \text{ mm}^2$ in area) in the granulator. Not only does this processing step take more time and energy, it is ineffective.
2. **Sifting:** Sifting successfully reduces the average particle area from 12.56 mm^2 to 9.14 mm^2 and shifts the particle size distribution curve to the left (Figure 6). This is a promising method for obtaining a printable granulate from rPET water bottles, but results in additional waste plastic.
3. **Heating:** Heating (a) at 65.5°C does not reduce particle area and instead slightly shifts the normal distribution curve to the right (Figure 4). This may indicate a loss of small particles in the dehydrator during the heating process, since the smallest particles can fall through the dehydrator's screen holes. However, heating (b) at 100°C in the oven does reduce particle area (Figure 4), presumably because the flat plastic particles curl and contract in

area while also increasing in thickness. The sample heated at 100°C also contained some particles that underwent a color change from clear to opaque white. The shape and color changes indicate crystallization of the amorphous PET water bottle plastic. Crystallization begins at the glass transition temperature (T_g), which for PET is in the range of 153°F - 178°F (67°C - 81°C) [72]. This explains why the shape and color changes were present in the PET heated at 100°C (above T_g) and not in the PET heated at 65°C (below T_g).

4. **Combined sifting and 100°C heating.** Finally, the combined approach was shown to further tighten the particle size distribution and shift it towards smaller particles as shown in Figure 6.

To investigate the impact of different water bottle sources on rPET properties when heated, squares cut from various brands of water bottles were heated at 100°C for 1 hour (Figure 7). After heating, their dimensions were measured while the squares were flat, and the percent change was found (Table 1).



Figure 7. Water bottle squares after 1 hour at 100°C (scale shown with 2 inch (50.8mm) white bar).

Table 1. 1" water bottle squares before and after a 1-hour heat cycle at 100°C

Bottle Brand	Post thermal treatment			Percent Change	
	Width (in)	Length (in)	Area (in ²)	Width	Length
Baraka	0.7	0.94	0.658	-30.0%	-6.0%
Hill Country Fare	0.87	0.91	0.7917	-13.0%	-9.0%
Great Value	0.84	0.96	0.8064	-16.0%	-4.0%
Ozarka	0.84	0.97	0.8148	-16.0%	-3.0%
Texas Music Water	0.88	0.97	0.8536	-12.0%	-3.0%

PET samples heated to 100°C underwent significant contractions in length and width across all water bottle brands. The sample squares contracted different amounts in each dimension, with an average percent change of -17.4% in one dimension and -5% in the other (Table 1). The difference between the two dimensions may be caused by the water bottle manufacturing process, but more investigation is needed to confirm. This indicates that heating above the glass transition temperature shows promising results in improving particle shape.

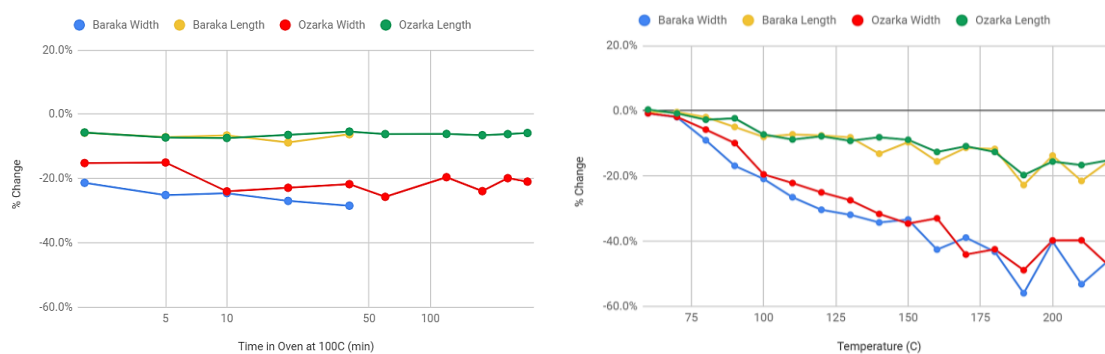


Figure 8: Effect of heating time (a) on dimensions (width and length) of 1" squares of PET water bottle plastic heated at 100°C (left) and (b) the effect of temperature on dimensions (width and length) of 1" squares of PET water bottle plastic heated for 5 minutes (right).

Heating tests for time dependency on PET sample dimension show that area reduction occurs within the first five minutes, and additional heating time does not provide additional particle shape benefits (Figure 8). By contrast, area reduces as temperature increases, beginning at the glass transition temperature (T_g) of PET. Area changes were similar across water bottle brands Baraka (avg thickness 0.25 mm) and Ozarka (average thickness 0.2 mm). These experiments also confirmed that the percent change in width was consistently double than that in length.

Based on conclusions from the temperature and time dependence tests, a sample of rPET water bottle flake was sifted, then heated at 190°C for 5 minutes to obtain a sample with the smallest cross-sectional particle area (Figure 9 as compared to results in Figure 6).

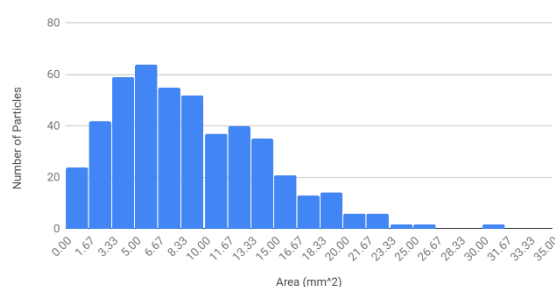


Figure 9. Particle size distribution of rPET water bottle flake sifted, then heated at 190°C for 5 minutes.

Although the combined sifting and heating at 190°C had the best chance of providing a functional material for the Gigabot X, the feeding tests showed that it was still incompatible. Although the Ultrafuse rPET pellets were easily fed through feed throat and 1" tubing, the processed samples of PET water bottle flake did not

consistently feed through the system. This severely impacted printability via the feed tube, and future work is needed in this area.

In order to print recycled water bottle rPET flakes, the second approach was used where the material is directly fed into the system using a 3-D printed hopper mounted on the extruder, and cooling system shown in Figure 3. Without cooling rPET of both types (pellets and flakes) could print, but had sub-optimal resolution. Cooling using the system shown in Figure 3 enabled both rPET materials to be printed.

3.2 Thermal analysis

Figures 10 show the DSC curve for a sample of PET water bottle mW/mg as a function of temperature ($^{\circ}\text{C}$). The positive y axis indicates exothermic reactions, while downward designates endothermic reactions. The PET water bottle samples have endothermic peaks after approximately 250°C , which indicates a melting peak, showing that the PET flakes have a melting temperature of about 250°C , which is what is expected of PET resin [73].

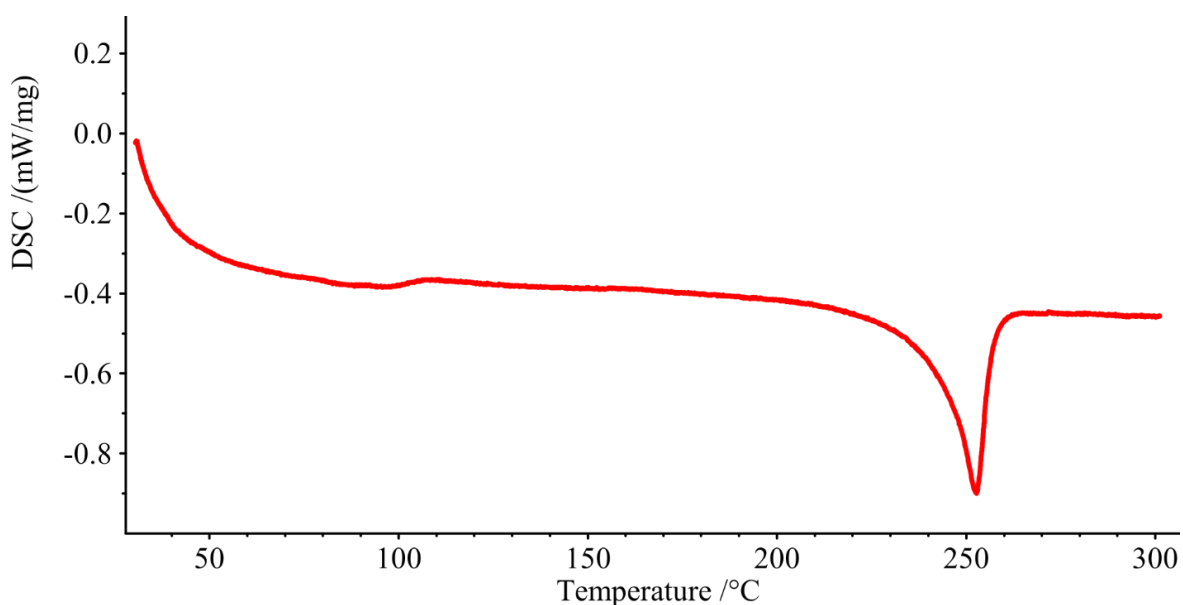


Figure 10. DSC curve of shredded water bottle.

3.3 3-D Printing

3.3.1 Optimization Results

The optimum temperature settings for 3-D printing were found for the approach shown in Figure 3 in Table 2 (details of all runs available in Appendix A). It should be noted, however, any specimen printed in the given temperature range was sufficiently good in visual quality and mass of print.

Table 2. Optimal print settings for the 3 temperature zones of the Gigabot X for no fan and small fan cases for rPET flake (Figure 3).

Cooling fan	Shape of print	Temperature (°C)		
		Bottom	Middle	Top
No Fan used	Cylinder	210	200	200
	Cuboid	230	230	220
SmallFan used	Cylinder	220	220	210
	Cuboid	230	220	220

Specimens printed at high speeds were consistently under-extruded for various temperatures. Hence a low speed of 10mm/s was chosen as the ideal print speed.

3.3.2 Mechanical testing

The average tensile strength of the rPET pellets printed with a cooling fan was 12.93MPa with a standard deviation of 4.72MPa, while the average tensile strength of the sample printed without using a cooling fan was 25.32MPa with a standard deviation of 5.82MPa. The use of a cooling fan clearly reduced the tensile strength of the specimen although it provided better resolution. It is also observed that the average mass of the sample printed using a cooling fan was 9.5 grams, while it was 9.2 grams without using a fan. The highest value observed is within the range previously reported for PET water bottles in a scientifically controlled environment [60]. PET has a bulk tensile strength of 47 to 90 MPa [74], whereas Zander et al., have shown 3-D printed PET ranged from 27 to 45 MPa [60]. Woern et al., have shown rPET in a Gigabot X prototype produced an average tensile strength was 40 MPa [61].

In addition, although rPET from flake was found to be printable via direct hopper, the lack of reproducibility and extreme brittleness resulted in an in nonviable print for tensile testing since it could not be removed from the build surface, as shown in Figure 11.



Figure 11. Tensile bar printed in rPET from water bottle flake fractured on bed removal.

Further study must be done to understand the reason for this observed brittleness of the rPET from water bottle flakes as well as the variable strength of

rPET pellets observed here although a few hypotheses can be made. First, the propensity of PET to break down in the presence of water and heat is well known. Although the PET was dried before entering the open hopper, the humidity in the room would have enabled access to water. Depending on the print order of the sample, the rPET plastic could have been held at elevated temperatures within the bore of the Gigabot X, partially breaking it down. This may indicate why previous results with a shorter two stage Gigabot X hot end (and thus a shorter high temperature residence time) resulted in higher tensile strengths for rPET [61]. This brings us to the second explanation - that the results indicate there is a wide variety in the quality of PET water bottle plastic and this plastic could have been of the less mechanically or chemically stable variety. The most perplexing result is that the strengths with cooling were roughly half those without cooling. This is not expected as a faster cooling rate would typically result in higher strength. The average mass with cooling was also larger by about 3%, which would have also indicated that it would be stronger. The nature of material extrusion-based 3-D printing may also help to explain this result. If the plastic coming out in both cases was roughly the same (or even slightly higher for the cooling fan case) yet the rapid cooling could create more interline spacing (triangular shaped air gaps) as previously observed in FFF printing [75] this would be expected to reduce strength even if the prints appeared solid. In addition, because the two cases that were tested for tensile strength were no cooling and modest cooling, slow print speeds were necessary (10 mm/s), which would be expected to increase any breakdown in the material.

3.3.3 Example Print

The three-heating stage Gigabot X beta, was able to fabricate several example prints with rPET pellets, although not from water bottle plastic because of the feeding issues discussed above. Despite the rPET being substantially weaker than injection molded PET, the values of 25 MPa are close to those observed for commercial FDM of ABS plastic as well as FFF ABS printed under realistic conditions [76]. This makes the rPET more than adequate for a number of applications. Several examples are shown for military tools and training aids in Figure 12: (A) Air Force training aid: Successfully printed with a 0.8 mm nozzle and no support; (B) KMZ topographical map: Printed first with a 1.75 mm nozzle, then a 0.8 mm nozzle to improve resolution; (C) Propeller: Printed with a 0.8 mm nozzle with support (surfaces contacting the support can be improved with higher resolution and dual extrusion); (D) Planning Tool: The combination of support and high-detail parts could not be achieved with the resolution from either the 1.75 or 0.8 mm nozzles; (E) Jet Engine jig to paint the white line on a spinner: Successfully printed with a 1.75 mm nozzle with vase mode. Overhanging edges can be further improved by a smaller nozzle and this would also solve the printing issues seen in Figure 12B.

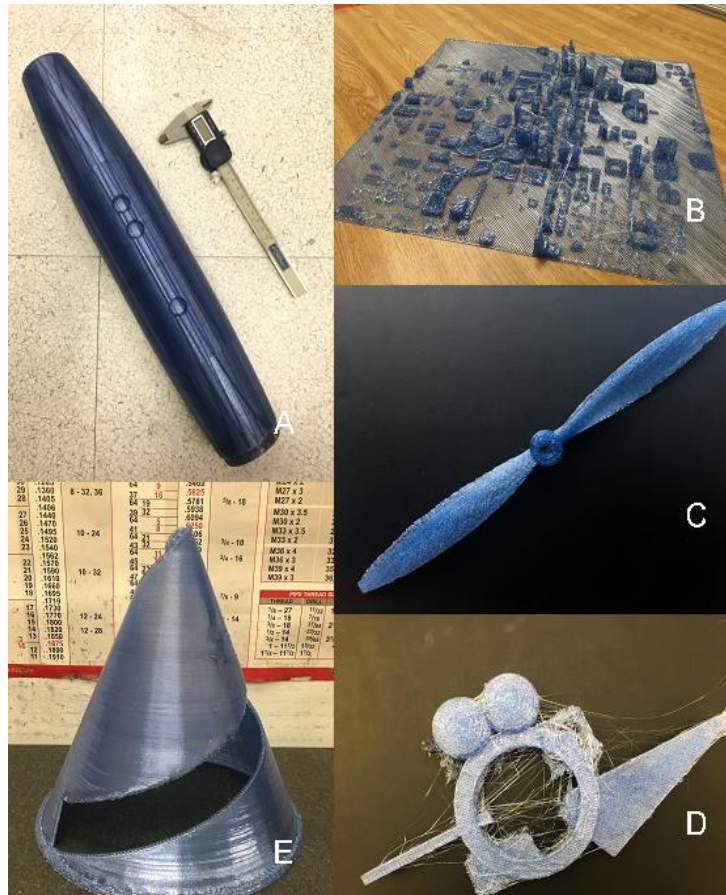


Figure 12 Example Gigabot X beta test prints: (A) Air Force training aid, (B) topographical map KMZ, (C) propeller, (D) planning tool, and (E) spinner.

To further demonstrate the feasibility of using rPET to print a high demand object [77–80], the Gigabot X was used to print a face shield as shown in Figure 13.



Figure 13. Recycled PET pellets used to print a face shield.

4. Future Work

This study has uncovered several areas of future work. First, improved methods of granulating PET from water bottles as well as processing rPET flake into an FPF/FGF machine is needed. This is expected to help feeding issues observed in this study with the Gigabot X feeding tube system which, unlike the hopper system, enables large-scale, long-term printing, and already works with uniform feedstocks like pellets. Future investigation into improving feeding issues for water bottle flake and similarly shaped recycled flake can include flake processing techniques, feed system part geometry to improve flow, and a motorized auger screw to physically pack particles into the extruder. Second, the results of this study showed there is a large difference in the rPET that comes from different waste streams as well as their processing history. This could be a function not only of the supplier and their feedstocks and additives, but could also be influenced by age of the waste, whether it was stored in direct sunlight, and the thermal history. This is a complex problem and a far more detailed study should be completed looking at rPET from many sources, locations in the world, and suppliers to provide optimal printing parameters for direct extrusion printers like the Gigabot X. One of the first steps could be the development of an open source melt flow index (MFI) device that could be used to rapidly screen rPET materials at a low cost. In order to overcome the slow printing speeds used in this study, a more powerful fan could be added to the system to enable rapid part cooling. This would be expected to allow for faster printing (reducing residence time and reducing material breakdown). Detailed study measuring the crystallinity of the printed specimen is required to understand the reason for the difference in tensile strength between specimens printed with and without a fan. In order to better understand the material breakdown, a careful study of residence time vs strength could be completed for future work. Finally, in order to ensure that the rPET remains dry a heated hopper/feeding unit could be investigated and would be expected to improve results. This work should enable rPET from water bottles to be used as a reliable feedstock for DRAM.

5. Conclusions

Although far from optimized, the results of this study show the potential to reach a circular economy for post-consumer recycled rPET as a DRAM feedstock when used with Gigabot X FPF/FGF 3-D printing. The results showed that extended feeding tubes were challenging with rPET flakes when processed by simple shredding, sifting, or heating (and the combination), but they could be directly printed using a hopper and resolution could be improved with active cooling. Further this study showed a wide disparity in the physical properties of rPET depending on source and indicated a large area for future work both in material characterization as well as processing and machine design to make rPET from water bottles a common feedstock.

Author Contributions: Conceptualization, Samantha L. Snabes and and Joshua M. Pearce; Data curation, Nagendra G. Tanikella and Matthew Reich; Formal analysis, Helen A. Little, Nagendra G. Tanikella, Matthew Reich, Matthew J. Fiedler, Samantha L. Snabes and and Joshua M. Pearce; Funding acquisition, Samantha L. Snabes and and Joshua M. Pearce; Investigation, Helen A. Little, Nagendra G. Tanikella and Matthew Reich; Methodology, Helen A. Little, Nagendra G. Tanikella and Matthew Reich; Project administration, and Joshua M. Pearce; Resources, and Joshua M. Pearce; Supervision, and Joshua M. Pearce; Validation, Helen A. Little and Matthew Reich; Visualization, Helen A. Little, Nagendra G. Tanikella and Matthew Reich; Writing – original draft, Helen A. Little and and Joshua M. Pearce; Writing – review & editing, Helen A. Little, Nagendra G. Tanikella, Matthew Reich, Matthew J. Fiedler, Samantha L. Snabes and and Joshua M. Pearce. All authors have read and agreed to the published version of the manuscript.

Funding: This research was funded by NSF SBIR Phase II grant number: 1746480 and the WeWork Global Creator Award.

Acknowledgments: The authors would like to thank Aubrey Woern and Samantha Reeve for helpful comments.

Conflicts of Interest: Helen A. Little, Matthew J. Fiedler and Samantha L. Snabes are employees of re:3D, which manufactures the Gigabot X that was used in this study. The authors from MTU have no conflict of interest. The funders played no part in the design of the study, in the collection, analyses, or interpretation of the data, in the writing of the manuscript, or in the decision to publish the results.

Appendix A.

A1 Small Fan- cylinder

PRINT OPTIMIZATION														
Details		Print Settings						Results Objective				Analysis Subjective		
Print	Trial	Temperature				Cooling fan (Small)	Speed (mm/s)	Completed Print?	Motor skip?	Mass (g)	Results Objective			Analysis Subjective
		Bottom (C)	Middle (C)	Top (C)	Bed (C)						Dis (mm) (Max)	Height (mm)	Appearance	
linder (D20°H	0.1	250	240	230	75	ON	10	Yes	No	13	20.46	38.89	Good	Slightly hot
linder (D20°H	0.2	250	240	230	75	ON	30				DNP			
linder (D20°H	0.3	250	240	230	75	ON	50	Yes	No	13.3	21.43	37.52	Bad	Too hot
linder (D20°H	0.4	220	210	200	75	ON	10	Yes	No	13.3	20.16	39.47	Good	Cold start, good later
linder (D20°H	0.5	220	210	200	75	ON	30				DNP			
linder (D20°H	0.6	220	210	200	75	ON	50				DNP			
linder (D20°H	0.7	200	190	180	75	ON	10				DNP			
linder (D20°H	0.8	200	190	180	75	ON	30				DNP			
linder (D20°H	0.9	200	190	180	75	ON	50				DNP			
New optimization temperatures		240		210										
Reason		Too hot at 250				Cold at 200								
linder (D20°H	1.1	240	240	230	75	ON	10				DNP			
linder (D20°H	1.2	240	230	230	75	ON	10				DNP			
linder (D20°H	1.3	240	230	220	75	ON	10				DNP			
linder (D20°H	1.4	230	230	220	75	ON	10				DNP			
linder (D20°H	1.5	230	220	220	75	ON	10	Yes	No	13.3	19.86	39.46	Good	Slightly Hot
linder (D20°H	1.6	230	220	210	75	ON	10	Yes	No	14	20.12	39.62	Good	Slightly Hot
linder (D20°H	1.7	220	220	210	75	ON	10	Yes	No	13.3	20.1	39.66	Good	Good print

A2 Small-FanLarge short cuboid.

PRINT OPTIMIZATION												
Details		Print Settings						Results Objective				Analysis Subjective
		Temperature			Cooling fan (Small)	Speed (mm/s)	Completed Print?	Motor skip?	Mass (g)	Height (mm)	Appearance	
Print	Trial	Bottom (C)	Middle (C)	Top (C)								
Cuboid (S50_H5)	0.1	260	250	240	ON	10	yes	no			Brittle	Too hot
Cuboid (S50_H5)	0.2	260	250	240	ON	30					DNP	
Cuboid (S50_H5)	0.3	260	250	240	ON	50	yes	no	Broken sample		Brittle	Too hot
Cuboid (S50_H5)	0.4	240	230	220	ON	10	yes	no	12.8	4.99	Brittle	Too hot
Cuboid (S50_H5)	0.5	240	230	220	ON	30	yes	no	13.2	4.68	good	Underextruded
Cuboid (S50_H5)	0.6	240	230	220	ON	50					DNP	
Cuboid (S50_H5)	0.7	220	210	200	ON	10	yes	no	14.5	4.78	good	Slightly Underextruded
Cuboid (S50_H5)	0.8	220	210	200	ON	30					DNP	
Cuboid (S50_H5)	0.9	220	210	200	ON	50					DNP	
low optimization temperature 230 210												
Reason 240 was too brittle/light underextrusion, 220 would probably work												
Cuboid (S50_H5)	1.1	230	230	220	ON	10	yes	no	14.7	4.92	Perfect	Good print
Cuboid (S50_H5)	1.2	230	220	220	ON	10	yes	no	15	5.09	Perfect	Good print
Cuboid (S50_H5)	1.3	230	220	210	ON	10	yes	no	14.7	4.92	Perfect	Good print

A3. No fan small tall cylinder

PRINT OPTIMIZATION																							
Details		Print Settings						Results Objective				Analysis Subjective											
		Temperature			Cooling fan (Small)	Speed (mm/s)	Retraction (mm)	Restart Distance (mm)	Coasting (mm)	Constants	Completed Print?	Motor skip?	Mass (g)	Dia (mm)	Height (mm)	Appearance							
Print	Trial	Bottom (C)	Middle (C)	Top (C)														Bed (C)					
linder (D20"H	0.1	280	240	230	75	OFF	30	1	0.5	3	retraction	No	No			DNP							
linder (D20"H	0.2	175	1	Auto	1	100	250	240	230	75	OFF	30	1	0.5	3	speed							
linder (D20"H	0.3	175	1	Auto	1	100	250	240	230	75	OFF	50	1	0.5	3	(11.7);	Yes	No	13.5	22.48	38.92	Bad	Too hot
linder (D20"H	0.4	175	1	Auto	1	100	220	210	200	75	OFF	30	1	0.5	3	vertical lift	Yes	No				DNP	
linder (D20"H	0.5	175	1	Auto	1	100	220	210	200	75	OFF	30	1	0.5	3	(0);	Yes	Minimal	14.2	21.86	39.02	Almost good	Too hot
linder (D20"H	0.6	175	1	Auto	1	100	220	210	200	75	OFF	50	1	0.5	3	Shells,top,b	Yes	Minimal	14.2	21.86	39.02	Almost good	Too hot
linder (D20"H	0.7	175	1	Auto	1	100	200	190	180	75	OFF	10	1	0.5	3	ottom: 2;	Yes	Yes, severe	7.4	18.7	39.37	Bad	Too cold
linder (D20"H	0.8	175	1	Auto	1	100	200	190	180	75	OFF	30	1	0.5	3	Start	Yes	Minimal	12.9	20.32	38.68	Best	Good print
linder (D20"H	0.9	175	1	Auto	1	100	200	190	180	75	OFF	50	1	0.5	3	location:	Yes	Moderate	13	20.25	39.16	Better	Good print
New optimization temperatures 210 200																							
Reason Print was almost good at trial 6 (speed), but too severely at 180, minimally at 200																							
linder (D20"H	1.1	175	1	Auto	1	100	210	210	200	75	OFF	10	1	0.5	3	retraction	Yes	No	13.2	21.5	38.75	Good	Too hot
linder (D20"H	1.2	175	1	Auto	1	100	210	210	200	75	OFF	30	1	0.5	3	speed						DNP	
linder (D20"H	1.3	175	1	Auto	1	100	210	210	200	75	OFF	50	1	0.5	3	(11.7);	Yes	Minimal	13.2	21.3	38.8	Almost good	Too hot
linder (D20"H	1.4	175	1	Auto	1	100	210	200	200	75	OFF	10	1	0.5	3	vertical lift	Yes	Minimal	13.4	20.4	38.85	Best	Good print
linder (D20"H	1.5	175	1	Auto	1	100	210	200	200	75	OFF	30	1	0.5	3	(0);	Yes	Minimal	12.9	20.32	38.68	Best	Good print
linder (D20"H	1.6	175	1	Auto	1	100	210	200	200	75	OFF	50	1	0.5	3	Shells,top,b	Yes	Minimal	13.1	20.9	38.03	Good	Too hot
linder (D20"H	1.7	175	1	Auto	1	100	200	200	200	75	OFF	10	1	0.5	3	ottom: 2;	Yes	Minimal	13.4	20.4	38.85	Best	Good print
linder (D20"H	1.8	175	1	Auto	1	100	200	200	200	75	OFF	30	1	0.5	3	Start:	Yes	Moderate	13	20.25	39.16	Better	Good print
linder (D20"H	1.9	175	1	Auto	1	100	200	200	200	75	OFF	50	1	0.5	3	location:						DNP	

A3 No fan large short cuboid

PRINT OPTIMIZATION																							
Details		Print Settings						Results Objective				Analysis Subjective											
		Temperature			Cooling fan (Small)	Speed (mm/s)	Retraction (mm)	Restart Distance (mm)	Coasting (mm)	Constants	Completed Print?	Motor skip?	Mass (g)	Height (mm)	Appearance								
Print	Trial	Bottom (C)	Middle (C)	Top (C)													Bed (C)						
Cuboid (S50_H5)	0.1	175	1	Auto	1	100	280	240	240	75	OFF	10	1	0.5	3	retraction	yes	no	13.3	4.17		Brittle	Too hot
Cuboid (S50_H5)	0.2	175	1	Auto	1	100	260	250	240	75	OFF	30	1	0.5	3	speed						DNP	
Cuboid (S50_H5)	0.3	175	1	Auto	1	100	260	250	240	75	OFF	50	1	0.5	3	(11.7);	yes	no				Shattered	Too hot
Cuboid (S50_H5)	0.4	175	1	Auto	1	100	240	230	220	75	OFF	10	1	0.5	3	vertical lift	yes	no	14.5	4.65		Better	Good Print
Cuboid (S50_H5)	0.5	175	1	Auto	1	100	240	230	220	75	OFF	30	1	0.5	3	(0);	yes	no	13.3	4.68		Good	Slightly underextruded
Cuboid (S50_H5)	0.6	175	1	Auto	1	100	240	230	220	75	OFF	50	1	0.5	3	Shells,top,b	yes	no	11.7	4.98		Almost good	Under extrusion
Cuboid (S50_H5)	0.7	175	1	Auto	1	100	220	210	200	75	OFF	10	1	0.5	3	ottom: 2;	yes	no	13.6	4.8		Good	Good Print
Cuboid (S50_H5)	0.8	175	1	Auto	1	100	200	210	200	75	OFF	30	1	0.5	3	Start	yes	no	13.9	4.68		Good	Good Print
Cuboid (S50_H5)	0.9	175	1	Auto	1	100	220	210	200	75	OFF	50	1	0.5	3	location:	no	yes				DNP	Minimal Motor skipping
New optimization temperatures considered 10,30 only 230 210																							
Reason 240 printed with Minimal skipping at 200 can be avoided																							
Cuboid (S50_H5)	1.1	175	1	Auto	1	100	230	230	220	75	OFF	10	1	0.5	3	retraction	yes	no	14.2	4.92		Better	Good Print
Cuboid (S50_H5)	1.2	175	1	Auto	1	100	230	230	220	75	OFF	30	1	0.5	3	speed	yes	no	13.8	4.67		Better	Good Print
Cuboid (S50_H5)	1.3	175	1	Auto	1	100	230	220	220	75	OFF	10	1	0.5	3	(11.7);	yes	no	13.6	4.68		Better	Good Print
Cuboid (S50_H5)	1.4	175	1	Auto	1	100	230	220	220	75	OFF	30	1	0.5	3	vertical lift	yes	no	12.9	4.48		Good	Slightly underextruded
Cuboid (S50_H5)	1.5	175	1	Auto	1	100	230	220	210	75	OFF	10	1	0.5	3	(0);	yes	no	13.9	4.61		Better	Slightly underextruded
Cuboid (S50_H5)	1.6	175	1	Auto	1	100	230	220	210	75	OFF	30	1	0.5	3	Shells,top,b						DNP	

References

- Geyer, R.; Jambeck, J.R.; Law, K.L. Production, use, and fate of all plastics ever made. *Sci. Adv.* **2017**, *3*, e1700782, doi:10.1126/sciadv.1700782.
- Brooks, A.L.; Wang, S.; Jambeck, J.R. The Chinese import ban and its impact on global plastic waste trade. *Sci. Adv.* **2018**, *4*, eaat0131, doi:10.1126/sciadv.aat0131.
- Katz, C. Piling Up: How China's Ban on Importing Waste Has Stalled Global Recycling Available online: <https://e360.yale.edu/features/piling-up-how-chinas-ban-on-importing-waste-has-stalled-global-recycling> (accessed on May 8, 2020).
- McNaughton, S. How China's plastic waste ban forced a global recycling reckoning Available online: <https://www.nationalgeographic.com/magazine/2019/06/china-plastic-waste-ban-impacting-countries-worldwide/> (accessed on May 8, 2020).
- Joyce, C. U.S. Recycling Industry Is Struggling To Figure Out A Future Without China Available online: <https://www.npr.org/2019/08/20/750864036/u-s-recycling-industry-is-struggling-to-figure-out-a-future-without-china> (accessed on May 8, 2020).
- Corkery, M. As Costs Skyrocket, More U.S. Cities Stop Recycling. *N. Y. Times* 2019.

7. Packaging Europe Pioneering sorting technology: HolyGrail project moves towards a circular economy Available online: <https://packagingeurope.com/api/content/6c4a9c8e-81de-11e9-898c-12f1225286c6/> (accessed on May 8, 2020).
8. Geissdoerfer, M.; Savaget, P.; Bocken, N.M.P.; Hultink, E.J. The Circular Economy – A new sustainability paradigm? *J. Clean. Prod.* **2017**, *143*, 757–768, doi:10.1016/j.jclepro.2016.12.048.
9. Kirchherr, J.; Reike, D.; Hekkert, M. Conceptualizing the circular economy: An analysis of 114 definitions. *Resour. Conserv. Recycl.* **2017**, *127*, 221–232, doi:10.1016/j.resconrec.2017.09.005.
10. Stahel, W.R. The circular economy. *Nat. News* **2016**, *531*, 435, doi:10.1038/531435a.
11. Zhong, S.; Pearce, J.M. Tightening the loop on the circular economy: Coupled distributed recycling and manufacturing with recyclebot and RepRap 3-D printing. *Resour. Conserv. Recycl.* **2018**, *128*, 48–58, doi:10.1016/j.resconrec.2017.09.023.
12. Pavlo, S.; Fabio, C.; Hakim, B.; Mauricio, C. 3D-Printing Based Distributed Plastic Recycling: A Conceptual Model for Closed-Loop Supply Chain Design. In Proceedings of the 2018 IEEE International Conference on Engineering, Technology and Innovation (ICE/ITMC); 2018; pp. 1–8.
13. Cruz Sanchez, F.A.; Boudaoud, H.; Camargo, M.; Pearce, J.M. Plastic recycling in additive manufacturing: A systematic literature review and opportunities for the circular economy. *J. Clean. Prod.* **2020**, *264*, 121602, doi:10.1016/j.jclepro.2020.121602.
14. Gwamuri, J.; Wittbrodt, B.T.; Anzalone, N.C.; Pearce, J.M. *Reversing the Trend of Large Scale and Centralization in Manufacturing: The Case of Distributed Manufacturing of Customizable 3-D-Printable Self-Adjustable Glasses*; Social Science Research Network: Rochester, NY, 2014;
15. Wittbrodt, B.T.; Glover, A.G.; Laureto, J.; Anzalone, G.C.; Oppliger, D.; Irwin, J.L.; Pearce, J.M. Life-cycle economic analysis of distributed manufacturing with open-source 3-D printers. *Mechatronics* **2013**, *23*, 713–726, doi:10.1016/j.mechatronics.2013.06.002.
16. Petersen, E.E.; Pearce, J. Emergence of Home Manufacturing in the Developed World: Return on Investment for Open-Source 3-D Printers. *Technologies* **2017**, *5*, 7, doi:10.3390/technologies5010007.
17. Petersen, E.E.; Kidd, R.W.; Pearce, J.M. Impact of DIY Home Manufacturing with 3D Printing on the Toy and Game Market. *Technologies* **2017**, *5*, 45, doi:10.3390/technologies5030045.
18. Laplume, A.O.; Petersen, B.; Pearce, J.M. Global value chains from a 3D printing perspective. *J. Int. Bus. Stud.* **2016**, *47*, 595–609, doi:10.1057/jibs.2015.47.
19. Baechler, C.; DeVuono, M.; Pearce, J.M. Distributed recycling of waste polymer into RepRap feedstock. *Rapid Prototyp. J.* **2013**, *19*, 118–125, doi:10.1108/13552541311302978.
20. Woern, A.L.; McCaslin, J.R.; Pringle, A.M.; Pearce, J.M. RepRapable Recyclebot: Open source 3-D printable extruder for converting plastic to 3-D printing filament. *HardwareX* **2018**, *4*, e00026, doi:10.1016/j.ohx.2018.e00026.
21. Kreiger, M.; Anzalone, G.C.; Mulder, M.L.; Glover, A.; Pearce, J.M. Distributed Recycling of Post-Consumer Plastic Waste in Rural Areas. *MRS Online Proc. Libr. Arch.* **2013**, *1492*, 91–96, doi:10.1557/opl.2013.258.
22. Kreiger, M.A.; Mulder, M.L.; Glover, A.G.; Pearce, J.M. Life cycle analysis of distributed recycling of post-consumer high density polyethylene for 3-D printing filament. *J. Clean. Prod.* **2014**, *70*, 90–96, doi:10.1016/j.jclepro.2014.02.009.
23. Zhong, S.; Rakhe, P.; Pearce, J.M. Energy Payback Time of a Solar Photovoltaic Powered Waste Plastic Recyclebot System. *Recycling* **2017**, *2*, 10, doi:10.3390/recycling2020010.

24. Sells, E.; Bailard, S.; Smith, Z.; Bowyer, A.; Olliver, V. RepRap: The Replicating Rapid Prototyper: Maximizing Customizability by Breeding the Means of Production. In *Handbook of Research in Mass Customization and Personalization*; World Scientific Publishing Company, 2009; pp. 568–580 ISBN 978-981-4280-25-9.
25. Jones, R.; Haufe, P.; Sells, E.; Iravani, P.; Olliver, V.; Palmer, C.; Bowyer, A. RepRap – the replicating rapid prototyper. *Robotica* **2011**, *29*, 177–191, doi:10.1017/S026357471000069X.
26. Bowyer, A. 3D Printing and Humanity’s First Imperfect Replicator. *3D Print. Addit. Manuf.* **2014**, *1*, 4–5, doi:10.1089/3dp.2013.0003.
27. Hunt, E.J.; Zhang, C.; Anzalone, N.; Pearce, J.M. Polymer recycling codes for distributed manufacturing with 3-D printers. *Resour. Conserv. Recycl.* **2015**, *97*, 24–30, doi:10.1016/j.resconrec.2015.02.004.
28. Sanchez, F.A.C.; Lanza, S.; Boudaoud, H.; Hoppe, S.; Camargo, M. Polymer Recycling and Additive Manufacturing in an Open Source context: Optimization of processes and methods.; 2015; p. 1591.
29. Cruz Sanchez, F.A.; Boudaoud, H.; Hoppe, S.; Camargo, M. Polymer recycling in an open-source additive manufacturing context: Mechanical issues. *Addit. Manuf.* **2017**, *17*, 87–105, doi:10.1016/j.addma.2017.05.013.
30. Anderson, I. Mechanical Properties of Specimens 3D Printed with Virgin and Recycled Polylactic Acid. *3D Print. Addit. Manuf.* **2017**.
31. Pakkanen, J.; Manfredi, D.; Minetola, P.; Iuliano, L. About the Use of Recycled or Biodegradable Filaments for Sustainability of 3D Printing. In *Proceedings of the Sustainable Design and Manufacturing 2017*; Campana, G., Howlett, R.J., Setchi, R., Cimatti, B., Eds.; Springer International Publishing: Cham, 2017; pp. 776–785.
32. Mohammed, M.I.; Wilson, D.; Gomez-Kervin, E.; Tang, B.; Wang, J. Investigation of Closed-Loop Manufacturing with Acrylonitrile Butadiene Styrene over Multiple Generations Using Additive Manufacturing. *ACS Sustain. Chem. Eng.* **2019**, *7*, 13955–13969, doi:10.1021/acssuschemeng.9b02368.
33. Mohammed, M.I.; Wilson, D.; Gomez-Kervin, E.; Vidler, C.; Rosson, L.; Long, J. The Recycling of E-Waste ABS Plastics by Melt Extrusion and 3D Printing Using Solar Powered Devices as a Transformative Tool for Humanitarian Aid. 13.
34. Mohammed, M.I.; Wilson, D.; Gomez-Kervin, E.; Rosson, L.; Long, J. EcoPrinting: Investigation of Solar Powered Plastic Recycling and Additive Manufacturing for Enhanced Waste Management and Sustainable Manufacturing. In *Proceedings of the 2018 IEEE Conference on Technologies for Sustainability (SusTech)*; 2018; pp. 1–6.
35. Boldizar, A.; Möller, K. Degradation of ABS during repeated processing and accelerated ageing. *Polym. Degrad. Stab.* **2003**, *81*, 359–366, doi:10.1016/S0141-3910(03)00107-1.
36. Chong, S.; Pan, G.-T.; Khalid, M.; Yang, T.C.-K.; Hung, S.-T.; Huang, C.-M. Physical Characterization and Pre-assessment of Recycled High-Density Polyethylene as 3D Printing Material. *J. Polym. Environ.* **2017**, *25*, 136–145, doi:10.1007/s10924-016-0793-4.
37. Pepi, M.; Zander, N.; Gillan, M. Towards Expeditionary Battlefield Manufacturing Using Recycled, Reclaimed, and Scrap Materials. *JOM* **2018**, *70*, 2359–2364, doi:10.1007/s11837-018-3040-8.
38. Woern, A.L.; Pearce, J.M. Distributed Manufacturing of Flexible Products: Technical Feasibility and Economic Viability. *Technologies* **2017**, *5*, 71, doi:10.3390/technologies5040071.
39. Hart, K.R.; Frketic, J.B.; Brown, J.R. Recycling meal-ready-to-eat (MRE) pouches into polymer filament for material extrusion additive manufacturing. *Addit. Manuf.* **2018**, *21*, 536–543, doi:10.1016/j.addma.2018.04.011.

40. Reich, M.J.; Woern, A.L.; Tanikella, N.G.; Pearce, J.M. Mechanical Properties and Applications of Recycled Polycarbonate Particle Material Extrusion-Based Additive Manufacturing. *Materials* **2019**, *12*, 1642, doi:10.3390/ma12101642.
41. Oblak, P.; Gonzalez-Gutierrez, J.; Zupančič, B.; Aulova, A.; Emri, I. Processability and mechanical properties of extensively recycled high density polyethylene. *Polym. Degrad. Stab.* **2015**, *114*, 133–145, doi:10.1016/j.polymdegradstab.2015.01.012.
42. Lee, J.H.; Lim, K.S.; Hahm, W.G.; Kim, S.H. Properties of recycled and virgin poly(ethylene terephthalate) blend fibers. *J. Appl. Polym. Sci.* **2013**, *128*, 1250–1256, doi:10.1002/app.38502.
43. Tian, X.; Liu, T.; Wang, Q.; Dilmurat, A.; Li, D.; Ziegmann, G. Recycling and remanufacturing of 3D printed continuous carbon fiber reinforced PLA composites. *J. Clean. Prod.* **2017**, *142*, 1609–1618, doi:10.1016/j.jclepro.2016.11.139.
44. Parandoush, P.; Lin, D. A review on additive manufacturing of polymer-fiber composites. **2017**, doi:10.1016/j.compstruct.2017.08.088.
45. Heller, B.P.; Smith, D.E.; Jack, D.A. Planar deposition flow modeling of fiber filled composites in large area additive manufacturing. *Addit. Manuf.* **2019**, *25*, 227–238, doi:10.1016/j.addma.2018.10.031.
46. Pringle, A.M.; Rudnicki, M.; Pearce, J.M. Wood Furniture Waste–Based Recycled 3-D Printing Filament. *For. Prod. J.* **2017**, *68*, 86–95, doi:10.13073/FPJ-D-17-00042.
47. Zander, N.E. Recycled Polymer Feedstocks for Material Extrusion Additive Manufacturing. In *Polymer-Based Additive Manufacturing: Recent Developments*; ACS Symposium Series; American Chemical Society, 2019; Vol. 1315, pp. 37–51 ISBN 978-0-8412-3426-0.
48. Dertinger, S.C.; Gallup, N.; Tanikella, N.G.; Grasso, M.; Vahid, S.; Foot, P.J.S.; Pearce, J.M. Technical pathways for distributed recycling of polymer composites for distributed manufacturing: Windshield wiper blades. *Resour. Conserv. Recycl.* **2020**, *157*, 104810, doi:10.1016/j.resconrec.2020.104810.
49. Meyer, T.K.; Tanikella, N.G.; Reich, M.J.; Pearce, J.M. Potential of distributed recycling from hybrid manufacturing of 3-D printing and injection molding of stamp sand and acrylonitrile styrene acrylate waste composite. *Sustain. Mater. Technol.* **2020**, *25*, e00169, doi:10.1016/j.susmat.2020.e00169.
50. Zander, N.E.; Gillan, M.; Burckhard, Z.; Gardea, F. Recycled polypropylene blends as novel 3D printing materials. *Addit. Manuf.* **2019**, *25*, 122–130, doi:10.1016/j.addma.2018.11.009.
51. Awaja, F.; Pavel, D. Recycling of PET. *Eur. Polym. J.* **2005**, *41*, 1453–1477, doi:10.1016/j.eurpolymj.2005.02.005.
52. La Mantia, F.P. Polymer Mechanical Recycling: Downcycling or Upcycling? *Prog. Rubber Plast. Recycl. Technol.* **2004**, *20*, 11–24, doi:10.1177/147776060402000102.
53. Polyethylene Terephthalate Production, Price and Market – Plastics Insight Available online: <https://www.plasticsinsight.com/resin-intelligence/resin-prices/polyethylene-terephthalate/> (accessed on May 11, 2020).
54. Karayannidis, G.P.; Achilias, D.S. Chemical Recycling of Poly(ethylene terephthalate). *Macromol. Mater. Eng.* **2007**, *292*, 128–146, doi:10.1002/mame.200600341.
55. Nace, T. We're Now At A Million Plastic Bottles Per Minute - 91% Of Which Are Not Recycled Available online: <https://www.forbes.com/sites/trevornace/2017/07/26/million-plastic-bottles-minute-91-not-recycled/> (accessed on May 11, 2020).
56. B-Pet | Bottle PET Filament Available online: <https://bpetfilament.com/> (accessed on May 8, 2020).
57. RE PET 3D | Recycled PET filament.

58. Mosaddek, A.; Kommula, H.K.R.; Gonzalez, F. Design and Testing of a Recycled 3D Printed and Foldable Unmanned Aerial Vehicle for Remote Sensing. In Proceedings of the 2018 International Conference on Unmanned Aircraft Systems (ICUAS); 2018; pp. 1207–1216.
59. Refil | The makers of recycled filament | Order today Available online: <https://www.refilament.com/> (accessed on May 8, 2020).
60. Zander, N.E.; Gillan, M.; Lambeth, R.H. Recycled polyethylene terephthalate as a new FFF feedstock material. *Addit. Manuf.* **2018**, *21*, 174–182, doi:10.1016/j.addma.2018.03.007.
61. Woern, A.L.; Byard, D.J.; Oakley, R.B.; Fiedler, M.J.; Snabes, S.L.; Pearce, J.M. Fused Particle Fabrication 3-D Printing: Recycled Materials' Optimization and Mechanical Properties. *Materials* **2018**, *11*, 1413, doi:10.3390/ma11081413.
62. Alzahrani, M. Modification of Recycled Poly(ethylene terephthalate) for FDM 3D-Printing Applications. **2017**.
63. PET Facts | IBWA | Bottled Water Available online: <https://www.bottledwater.org/education/recycling/pet-facts> (accessed on May 11, 2020).
64. Parado-Guilford, C. Can recycled 3D printing filament lead to a successful social venture? Available online: <https://blogs.worldbank.org/digital-development/can-recycled-3d-printing-filament-lead-successful-social-venture> (accessed on May 11, 2020).
65. techfortrade's Thunderhead PET Filament Extruder Technical Feasibility Study Available online: <http://www.refabdar.org/updates/2016/8/31/techfortrade-thunderhead-pet-filament-extruder-technical-feasibility-study> (accessed on May 11, 2020).
66. Low Speed Open Rotor Scissor Cut Granulators | Shini USA 2016.
67. ImageJ Available online: <https://imagej.nih.gov/ij/download.html> (accessed on May 8, 2020).
68. Circularity Available online: <https://imagej.nih.gov/ij/plugins/circularity.html> (accessed on May 13, 2020).
69. Ultrafuse rPET Natural Blue. Available online: <https://www.ultrafusefff.com/product-category/sustainable/innocircle/> (accessed on May 13, 2020).
70. GigabotX OS cooling system. Available online: <https://osf.io/q2bkdl/> (visited July 28, 2020)
71. Lab, Q. Laboratory Ovens & Incubators Available online: <https://quincylab.com/analog-lab-ovens> (accessed on May 14, 2020).
72. Demirel, B.; Yaraş, A.; Elçiçek, H. Crystallization behavior of PET materials. *PET malzemelerin kristalizasyon davranışı* **2011**.
73. Resin Properties Table | PMC Available online: <https://www.pmcplastics.com/materials/pet-resin/> (accessed on May 19, 2020).
74. Overview of materials for Polyethylene Terephthalate (PET), Unreinforced Available online: <http://www.matweb.com/search/DataSheet.aspx?MatGUID=a696bdcdf6f41dd98f8eec3599eaa20&ckck=1> (accessed on May 13, 2020).
75. Wittbrodt, B.; Pearce, J.M. The effects of PLA color on material properties of 3-D printed components. *Addit. Manuf.* **2015**, *8*, 110–116, doi:10.1016/j.addma.2015.09.006.
76. Tymrak, B.M.; Kreiger, M.; Pearce, J.M. Mechanical properties of components fabricated with open-source 3-D printers under realistic environmental conditions. *Mater. Des.* **2014**, *58*, 242–246, doi:10.1016/j.matdes.2014.02.038.
77. Pearce, J. Distributed Manufacturing of Open-Source Medical Hardware for Pandemics. **2020**, doi:10.20944/preprints202004.0054.v1.

78. Tino, R.; Moore, R.; Antoline, S.; Ravi, P.; Wake, N.; Ionita, C.N.; Morris, J.M.; Decker, S.J.; Sheikh, A.; Rybicki, F.J.; et al. COVID-19 and the role of 3D printing in medicine. *3D Print. Med.* **2020**, *6*, 11, s41205-020-00064–7, doi:10.1186/s41205-020-00064-7.
79. Livingston, E.; Desai, A.; Berkwits, M. Sourcing Personal Protective Equipment During the COVID-19 Pandemic. *JAMA* **2020**, *323*, 1912–1914, doi:10.1001/jama.2020.5317.
80. Ishack, S.; Lipner, S.R. Applications of 3D Printing Technology to Address COVID-19 Related Supply Shortages. *Am. J. Med.* **2020**, doi:10.1016/j.amjmed.2020.04.002.